processes

MDPI

Article

Adaptive Fuzzy Fractional Order Global Sliding Mode Tracking Control Algorithm for Particleboard Glue System

Liangkuan Zhu *, Xing Qi and Peiyu Wang

College of Electrical Mechanical Engineering, Northeast Forestry University, Harbin 150040, China; dach05012@126.com (X.Q.); pywang1_11@163.com (P.W.)
* Correspondence: zhulk@126.com

Abstract: In this paper, a novel flow tracking control scheme for particleboard glue system with complex disturbance and unmeasurable system state is investigated. The method is based on hyperbolic tangent extended state observer and adaptive fuzzy fractional order global sliding mode control with exponential reaching law. The novel compound control scheme has the following advantages: Firstly, the extended state observer with hyperbolic tangent function can improve the estimation ability for the system state and complex disturbance without detailed knowledge of the controlled plant and disturbance model. Secondly, the global sliding mode control method based on fractional calculus can improve the response speed and robustness of the system, and provide a more flexible controller structure than the traditional sliding mode controller. Thirdly, the adaptive fuzzy controller is introduced to approximate the sliding mode switching term, so as to reduce the chattering phenomenon of the system. In addition, the convergence of the proposed observer and asymptotic stability of the control system are verified based on strict Lyapunov analysis. Finally, the numerical simulation results show the effectiveness of the proposed compound control scheme for particleboard glue system.

Keywords: particleboard glue system; hyperbolic tangent extended state observer; fractional order; global sliding mode control algorithm; complex disturbance

Citation: Zhu, L.; Qi, X.; Wang, P. Adaptive Fuzzy Fractional Order Global Sliding Mode Tracking Control Algorithm for Particleboard Glue System. *Processes* **2022**, *10*, 719. https://doi.org/10.3390/pr10040719

Academic Editor: Jean-Pierre Corriou

Received: 4 March 2022
Accepted: 4 April 2022
Published: 8 April 2022

1. Introduction

In recent years, the excessive exploitation of natural forests and the huge waste in the wood processing industry have led to an increasing use of particleboard as a substitute for wood resources [1]. As one of the three types of wood-based panels, particleboard uses small pieces of wood, residues or other plant straws produced during wood processing as raw materials, which provides a new direction for the development of wood-based panels [2]. Under the trend of global shortage of log resources, it is of great significance to meet the contradiction between supply and demand of high-quality wood resources and realize the benign development of the ecological environment through the particleboard industry.

The production process of particleboard mainly includes five sections: shavings preparation, drying and sorting, glue mixing and dosing, slab paving and hot pressing, and post-treatment [3]. As one of the important indicators of the level of particleboard production technology, whether the glue mixing and dosing section can achieve an accurate proportion is an index to measure the performance of the system. Under the same production process conditions, too much glue will lead to high water content of the shavings, which leads to foaming and increase the amount of formaldehyde released; too little glue will reduce the plasticity of the shavings and weaken the physical properties of the product [4]. Therefore, the quality of particleboard products strictly depends on the control performance of the glue dispensing system.

The glue control system of particleboard mainly changes the practical glue flow amount according to the flow rate of shavings. Due to factors such as the inertia of motor and pump, the distance and temperature of glue conveying pipeline, etc., it is often

an uncertain system with time delay, complex disturbance and unpredictable states [5]. There are many control methods to solve this kind of system, including proportional-integral-derivative (PID) control [6,7], active disturbance rejection control [8], sliding mode control [9–11], backstepping control [12], predictive control [13], neural network [14,15], etc. Sliding mode control, one of the most effective control strategies for the complex disturbance and uncertainty of the system, is widely used in motion control systems. In reference [16], an integral-type terminal sliding mode method based on adaptive compensation is proposed for the attitude and position finite-time tracking control of a quadrotor UAV subject to model uncertainties and external disturbances. Hu presented a new control method for dynamically positioning vessel by combining the idea of sliding mode control and estimation of uncertain disturbances in reference [17], which is used to suppress the influence of uncertain modeling and unknown disturbances in the system. However, the characteristics of sliding mode control determine that it inevitably has chattering problems, and how to weaken its influence is also one of the important research directions.

There are numerous algorithms to reduce chattering phenomena, such as neural networks, fuzzy logic and other optimization algorithms [18–21]. Due to its powerful universal approximation ability, fuzzy control strategy is applied to the approximation of many unknown parameters and nonlinear terms of the system to enhance the applicability of the system, which has been confirmed in the literature [22–24]. Although the traditional sliding mode controller can properly reduce the influence of system parameter uncertainty and external disturbance, how to improve the robustness of the whole process of the system is also another important issue.

To improve the global robustness and dynamic performance, global sliding mode control has been studied by a large number of scholars to solve the control problem of uncertain systems [25–28]. In reference [25], a global smooth sliding mode controller is proposed for a flexible air-breathing hypersonic vehicle to address actuator faults and parameter uncertainty. Furthermore, it designs a new fast finite-time high-order regulator to ensure finite-time convergence without singular states. For the tracking problem of a class of uncertain nonlinear systems, reference [26] proposes a global time-varying sliding mode control scheme with a predetermined convergence time, which the adaptive law is used to overcome the influence of system uncertainties and external disturbances. In reference [27], a new control method for nonlinear antilock braking system is proposed, which mainly introduces nonlinearity into the design of the global sliding mode surface to eliminate the arrival phase and ensure the robustness of the entire control process. A novel global equivalent sliding mode controller for bridge crane system is proposed in [28], which introduced a new switching function to weaken the chattering and realized the anti-sway positioning control under the condition of model parameter uncertainty and external disturbance.

Fractional-order calculus is an extension of integer-order calculus, which can effectively improve the performance of sliding mode controllers by using its rich parameter adjustable range and better information memory [29–32]. In view of this, fractional-order sliding mode control strategies have been studied by many scholars [33–36]. In order to enhance output power quality of a permanent magnet synchronous generator, a fractional order sliding mode control is proposed in reference [33]. In reference [34], an adaptive fractional-order terminal sliding mode controller is designed for crane control with uncertainties and unknown disturbances. Reference [35] studied the position tracking control of servo system with external disturbance, and proposed a fractional-order sliding mode control strategy based on nonlinear disturbance observer. Wu presented a design method about adaptive fractional-order non-singular terminal sliding mode control for the omni-directional mobile robot manipulator in reference [36], where the dynamic uncertainty of the system is estimated by fuzzy wavelet neural networks. Although the fractional-order sliding mode controller can improve the control accuracy and robustness of the system, it is worth noting that the good performance of the above methods relies on the accuracy of the system state signal measurement. However, due to the difficulty of measurement

implementation and high economic cost, sliding mode control still has certain limitations and challenges in engineering applications.

To solve these problems, some scholars have proposed control methods based on extended state observers [37–40]. In reference [37], a robust control laws based on the back-stepping sliding mode control and extended state observer are designed for pressure regulation of the oxygen mask in an oxygen supply system. Reference [38] presented a nonlinear extended state observer to estimate both disturbances and states of the double-joint manipulator system, which improves the control accuracy of the system. A nonlinear extended state observer constructed from piece-wise smooth functions consisted of linear and fractional power functions is proposed in reference [39] to improve the estimation accuracy. In an attempt to estimate and compensate the lump model uncertainties, reference [40] designed an extended state observer by using the hyperbolic tangent function and fully proved in Lyapunov framework that all closed-loop signals invariably keep bounded and the attitude tracking error ultimately converges to a little neighborhood of zero.

In previous work shown in reference [4,5], we designed an active disturbance rejection control (ADRC) algorithm and a dynamic surface control (DSC) strategy to study the disturbance rejection capability and transient performance of the particleboard glue system, respectively. Motivated by the above discussions, this study focuses on the global robustness of the system and observer improvements. The main contributions of this paper can be summarized as:

1. A novel hyperbolic tangent extended state observer is designed to estimation the system state and total disturbance in real time and compensate it to the controller.
2. A fractional order global sliding mode controller is designed by introducing fractional calculus, and the chattering phenomenon of the system is weakened by adaptive fuzzy logic control to improve the dynamic performance of the system. Combined with the above designed observer, a compound control strategy is introduced to solve the problems of model uncertainty, complex disturbance and unmeasurable system state in particleboard glue system.

The paper is organized as follows: In Section 2, the process of particleboard glue dosing is described and the state equation of the system is given. In Section 3, hyperbolic tangent extended state observer and the compound fractional order global sliding mode controller, based on adaptive fuzzy switching term approximator are introduced, and the stability of the system are verified in in Section 4. Simulation results of applying the compound controller are shown in Section 5, and the paper is ended with conclusions in Section 6.

2. Process and System Description

In the process of particleboard production, the main task of the glue dosing section is to control the application amount of glue by allocating the ratio of wood shavings to adhesive, so that the glue is evenly distributed on the wood shavings. The particleboard glue system is shown in Figure 1. It consists of a wood shavings supply device, a glue supply device and a mixing device. The screw bin and belt weighting device transport the wood shavings raw materials produced by the shavings supply device to the mixing device. The weighting sensor B and the rotary encoder are used to measure the weight of the particleboard on the belt and the rotation speed of the belt in real time. The glue supply device consists of raw glue tank, glue control pump and flowmeter. After receiving the signal of wood shavings measured by weighting sensor B, the control system calculates the corresponding instantaneous glue flow value according to the preset wood shavings-glue ratio, and further determines the speed of glue pump according to the relationship between motor speed and glue flow, thus realizing accurate tracking of glue flow to wood shavings flow in proportion. The mixing device is mainly used to realize the uniform mixing of wood shavings and adhesive.

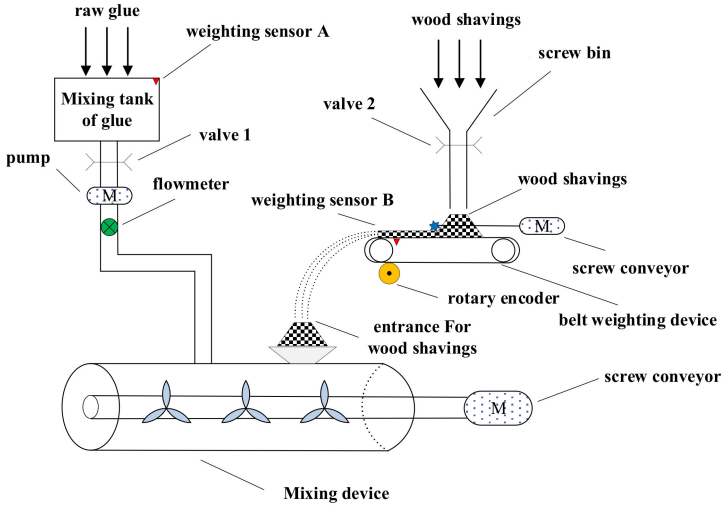

Figure 1. The schematic diagram of particleboard glue system.

The basic structure of a commonly used closed-loop control system for particleboard glue flow is shown in Figure 2. The practical flow value obtained by the electromagnetic flowmeter is compared with the ideal flow value, and then the error is sent to the controller. In order to reduce the error, the controller constantly adjusts the frequency of the converter to change the motor speed, so that the practical flow output by the glue pump is equal to the ideal flow.

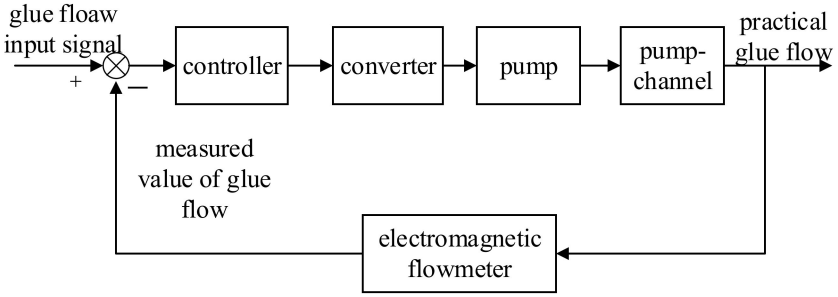

Figure 2. The basic structure of closed-loop control system for glue flow.

Due to the influence of the distance of glue conveying pipeline, the inertia of motor and pump, the glue dosing process is often a high-order inertial system with time delay. This often makes the closed-loop control system have larger overshoot and longer adjustment time. The transfer function of high-order inertial system with time delay can be described as:

$$G(s) = G_0(s)e^{-\tau s} = \frac{b}{s^n + a_{n-1}s^{n-1} + \cdots + a_1 s + a_0}e^{-\tau s}, \quad (1)$$

where $G_0(s)$ represents the part of the system without lag link, τ is the time lag constant, b, $a_{n-1}, \cdots, a_1, a_0$ is the system parameter.

For this kind of complex industrial object with time lag, it is often simplified as a first-order time-delay system (FOPTD) or a second-order time-delay system (SOPTD) in engineering. The two approximate models are shown in Equations (2) and (3), respectively.

$$G_{FOPTD} = \frac{K}{Ts + 1}e^{-\tau s}, \quad (2)$$

$$G_{SOPTD} = \frac{K}{s^2 + 2\xi\omega_n s + \omega_n^2}e^{-\tau s}, \quad (3)$$

In most cases, the system needs to meet the condition, $T > 0$, $\xi > 0$, $\omega_n > 0$, which means that all poles of the system are stable, otherwise the control problem of the system will become extremely challenging. The model of FOPTD is not applicable to all industrial processes, while SOPTD can be widely applied to accurate models of high-order systems. Considering the complexity of the actual industrial environment, we built an experimental system as shown in Figure 3 to simulate the actual industrial process.

Figure 3. The particleboard glue control device.

According to the literature [41], using the input and output data measured in the system experiment and operation, the system model obtained through identification is as follows:

$$G(s) = \frac{0.0209}{s^2 + 0.2584s + 0.0209} e^{-2.65s}, \tag{4}$$

Approximate the time-delay link $e^{-2.65s}$ to the first order inertial link $\frac{1}{2.65s+1}$, the transfer function model of the system in Equation (4) becomes:

$$\begin{aligned} G(s) &= \frac{0.0209}{s^2+0.2584s+0.0209} \cdot \frac{1}{2.65s+1} \\ &= \frac{0.0079}{s^3+0.6358s^2+0.1184s+0.0079} \end{aligned} \tag{5}$$

Considering the influence of parameter perturbation and external disturbance, the state equation of the system can be described as:

$$\begin{cases} \dot{x}_1 = x_2 \\ \dot{x}_2 = x_3 \\ \dot{x}_3 = f(x_1, x_2, x_3) + bu + \omega(t) \\ y = x_1 \end{cases}, \tag{6}$$

where $x = \begin{bmatrix} x_1 & x_2 & x_3 \end{bmatrix}^T$ is the state variables of the system, $f(x_1, x_2, x_3) = -0.0079x_1 - 0.1184x_2 - 0.6538x_3$ is the known information of the system model, $b = 0.0079$, $\omega(t) = \Delta f(x_1, x_2, x_3) + d(t)$ is the disturbance of the system, where $\Delta f(x_1, x_2, x_3)$ and $d(t)$ represent parameter perturbation and external disturbance, respectively.

Assumption 1. *$g(x_1, x_2, x_3, \omega(t), t) = \omega(t) + f(x_1, x_2, x_3)$ is an unknown continuously differentiable vector, which represents total disturbance of system, and $\left|\dot{g}(x_1, x_2, x_3, \omega(t), t)\right| \leq M$ where $\omega(t)$ is bounded.*

3. Design of the Compound Controller

In this section, a hyperbolic tangent extended state observer is proposed to estimate the state and total disturbance information of the system. On this basis, a fractional order global sliding mode controller is designed, and adaptive fuzzy control is used to approximate the sliding mode switching term. The structure diagram of adaptive fuzzy fractional order global sliding mode control based on a hyperbolic tangent extended state observer is shown in Figure 4.

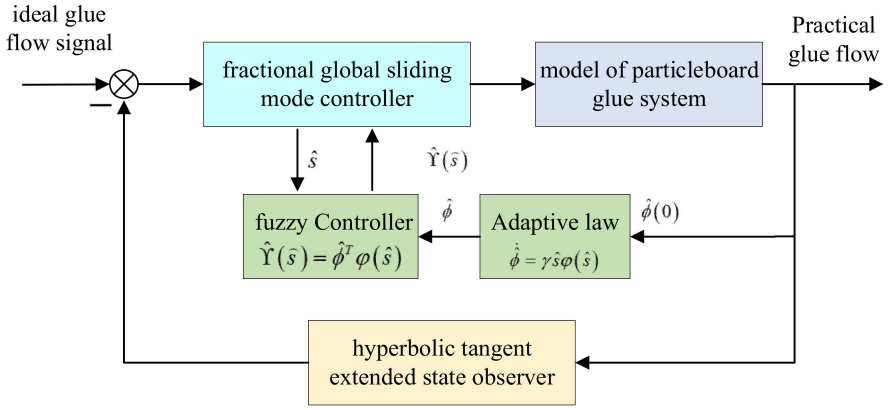

Figure 4. The structure diagram of adaptive fuzzy fractional order global sliding mode control based on hyperbolic tangent extended state observer.

3.1. Design of Hyperbolic Tangent Extended State Observer

Aiming at the problems of an unmeasurable state, parameter perturbation and external disturbance in particleboard glue system, combined with the idea of extended state observer, the disturbance $\omega(t)$ and known model information $f(x_1, x_2, x_3)$ are taken as new unknown state variable x_4 of the system, as shown in Equation (7):

$$x_4 = g(x_1, x_2, x_3, \omega(t), t) = \omega(t) + f(x_1, x_2, x_3), \tag{7}$$

Then, the equation of state (6) becomes:

$$\begin{cases} \dot{x}_1 = x_2 \\ \dot{x}_2 = x_3 \\ \dot{x}_3 = x_4 + bu \\ \dot{x}_4 = \dot{g}(x_1, x_2, x_3, \omega(t), t) \\ y = x_1 \end{cases}, \tag{8}$$

The hyperbolic tangent extended state observer designed for the system shown as Equation (8) is as follows:

$$\begin{cases} \varepsilon_1 = z_1 - y \\ \dot{z}_1 = z_2 - l_1 \tanh\left(\frac{\varepsilon_1}{\delta_1}\right) \\ \dot{z}_2 = z_3 - l_2 \tanh\left(\frac{\varepsilon_1}{\delta_2}\right) \\ \dot{z}_3 = z_4 - l_3 \tanh\left(\frac{\varepsilon_1}{\delta_3}\right) + bu \\ \dot{z}_4 = -l_4 \tanh\left(\frac{\varepsilon_1}{\delta_4}\right) \end{cases}, \tag{9}$$

where ε_1 represents glue flow tracking error, z_1, z_2 and z_3 are the estimated values of system states x_1, x_2 and x_3, respectively, z_4 is the estimated value of the total disturbance $g(x_1, x_2, x_3, \omega(t), t)$, $l_1 > 0$, $l_2 > 0$, $l_3 > 0$ and $l_4 > 0$ are the gain of extended state observer, $\delta_i > 0 (i = 1, 2, 3, 4)$ is the adjustable parameter that affects the estimation accuracy, $\tanh(\bullet)$ is hyperbolic tangent function.

The estimation error of hyperbolic tangent extended state observer is defined as:

$$\begin{cases} \tilde{\varepsilon}_1 = z_1 - x_1 \\ \tilde{\varepsilon}_2 = z_2 - x_2 \\ \tilde{\varepsilon}_3 = z_3 - x_3 \\ \tilde{\varepsilon}_4 = z_4 - x_4 \end{cases}, \tag{10}$$

Considering Equations (8)–(10), an estimated error system is given as follows:

$$\begin{cases} \dot{\tilde{\varepsilon}}_1 = \tilde{\varepsilon}_2 - l_1 \tanh\left(\frac{\tilde{\varepsilon}_1}{\delta_1}\right) \\ \dot{\tilde{\varepsilon}}_2 = \tilde{\varepsilon}_3 - l_2 \tanh\left(\frac{\tilde{\varepsilon}_1}{\delta_2}\right) \\ \dot{\tilde{\varepsilon}}_3 = \tilde{\varepsilon}_4 - l_3 \tanh\left(\frac{\tilde{\varepsilon}_1}{\delta_3}\right) \\ \dot{\tilde{\varepsilon}}_4 = -\dot{g} - l_4 \tanh\left(\frac{\tilde{\varepsilon}_1}{\delta_4}\right) \end{cases}, \tag{11}$$

Remark 1. *Using Taylor series for Hyperbolic tangent function, one may write:*

$$\begin{aligned} &\tanh\left(\frac{\tilde{\varepsilon}_1}{\delta_i}\right) = \frac{\tilde{\varepsilon}_1}{\delta_i} - \frac{(\tilde{\varepsilon}_1/\delta_i)^3}{3} + \frac{2(\tilde{\varepsilon}_1/\delta_i)^5}{15} - \frac{17(\tilde{\varepsilon}_1/\delta_i)^7}{315} + \cdots \\ &= \frac{\tilde{\varepsilon}_1}{\delta_i} - h\left(\frac{\tilde{\varepsilon}_1}{\delta_i}\right) \end{aligned} \tag{12}$$

where $h\left(\frac{\tilde{\varepsilon}_1}{\delta_i}\right) = \frac{(\tilde{\varepsilon}_1/\delta_i)^3}{3} - \frac{2(\tilde{\varepsilon}_1/\delta_i)^5}{15} + \frac{17(\tilde{\varepsilon}_1/\delta_i)^7}{315} - \cdots$, *and* $i = 1, 2, 3, 4$.

Then, the estimated error system becomes:

$$\dot{\tilde{\varepsilon}} = A\tilde{\varepsilon} + B\dot{g} + H, \tag{13}$$

where

$$\begin{aligned} A &= \begin{bmatrix} -l_1/\delta_1 & 1 & 0 & 0 \\ -l_2/\delta_2 & 0 & 1 & 0 \\ -l_3/\delta_3 & 0 & 0 & 1 \\ -l_4/\delta_4 & 0 & 0 & 0 \end{bmatrix}, B = \begin{bmatrix} 0 \\ 0 \\ 0 \\ -1 \end{bmatrix}, \\ H &= \begin{bmatrix} h\left(\frac{\tilde{\varepsilon}_1}{\delta_1}\right) & h\left(\frac{\tilde{\varepsilon}_1}{\delta_2}\right) & h\left(\frac{\tilde{\varepsilon}_1}{\delta_3}\right) & h\left(\frac{\tilde{\varepsilon}_1}{\delta_4}\right) \end{bmatrix}^T \end{aligned} \tag{14}$$

The characteristic equation of matrix A can be expressed as follows:

$$|\rho I - A| = \rho^4 + \frac{l_1}{\delta_1}\rho^3 + \frac{l_2}{\delta_2}\rho^2 + \frac{l_3}{\delta_3}\rho + \frac{l_4}{\delta_4}. \tag{15}$$

Theorem 1. *Considering the estimated error system (11), the estimated errors* $\tilde{\varepsilon}_1$, $\tilde{\varepsilon}_2$, $\tilde{\varepsilon}_3$ *and* $\tilde{\varepsilon}_4$ *are bounded by choosing appropriate parameters* l_1, l_2, l_3, l_4 *and* δ_1, δ_2, δ_3, δ_4 *which are satisfied with*

$$\frac{l_1 l_2}{l_3} > \frac{\delta_1 \delta_2}{\delta_3}, \tag{16}$$

$$l_1 l_2 l_3 \delta_1 \delta_3 \delta_4 > \delta_2 \left(l_3^2 \delta_1^2 \delta_4 + l_1^2 l_4 \delta_3^2\right). \tag{17}$$

That is, the estimated error system (11) is bounded stable.

Proof of Theorem 1. Choose the Lyapunov function for the observer as

$$V_o = \tilde{\varepsilon}^T \mathrm{X} \tilde{\varepsilon}. \tag{18}$$

If Equations (16) and (17) hold, then matrix A satisfies Hurwitz, and the derivative of V_o can be expressed as

$$\begin{aligned} \dot{V}_o &= \dot{\tilde{\varepsilon}}^T \mathrm{X} \tilde{\varepsilon} + \tilde{\varepsilon}^T \mathrm{X} \dot{\tilde{\varepsilon}} \\ &= \left(A\tilde{\varepsilon} + B\dot{g} + H\right)^T \mathrm{X} \tilde{\varepsilon} + \tilde{\varepsilon}^T \mathrm{X} \left(A\tilde{\varepsilon} + B\dot{g} + H\right) \\ &= \tilde{\varepsilon}^T \left(A^T \mathrm{X} + \mathrm{X} A\right) \tilde{\varepsilon} + 2\tilde{\varepsilon}^T \mathrm{X} B\dot{g} + 2\tilde{\varepsilon}^T \mathrm{X} H \end{aligned} \tag{19}$$

As matrix A satisfies Hurwitz, there is symmetric positive definite matrix Q satisfying

$$A^T \mathrm{X} + \mathrm{X} A = -Q. \tag{20}$$

According to Young's Inequality, the following inequality can be obtained:

$$2\tilde{\varepsilon}^T \mathrm{X} B\dot{g} \le \|\mathrm{X}\| \|\tilde{\varepsilon}\|^2 + \|\mathrm{X}\| \left\|B\dot{g}\right\|^2, \tag{21}$$

$$2\tilde{\varepsilon}^T \mathrm{X} H \le \|\mathrm{X}\| \|\tilde{\varepsilon}\|^2 + \|\mathrm{X}\| \|H\|^2. \tag{22}$$

Therefore, the derivative of V_o is rewritten as follows:

$$\begin{aligned} \dot{V}_o &= -\tilde{\varepsilon}^T Q \tilde{\varepsilon} + 2\tilde{\varepsilon}^T \mathrm{X} B\dot{g} + 2\tilde{\varepsilon}^T \mathrm{X} H \\ &\le -\rho_{\min}(Q) \|\tilde{\varepsilon}\|^2 + \|\mathrm{X}\| \|\tilde{\varepsilon}\|^2 + \|\mathrm{X}\| \left\|B\dot{g}\right\|^2 + \|\mathrm{X}\| \|\tilde{\varepsilon}\|^2 + \|\mathrm{X}\| \|H\|^2 \\ &\le \left[-\rho_{\min}(Q) + 2\|\mathrm{X}\|\right] \|\tilde{\varepsilon}\|^2 + \|\mathrm{X}\| \left(\left\|B\dot{g}\right\|^2 + \|H\|^2\right) \end{aligned} \tag{23}$$

where $\rho_{\min}(Q)$ represents the minimum eigenvalue of matrix Q. Note that $\rho_{\min}(Q) > 2\|\mathrm{X}\|$ is ensured by selecting the adjustable parameters l_1, l_2, l_3, l_4 and δ_1, δ_2, δ_3, δ_4, which are satisfied with inequalities in Equations (16) and (17). According to the condition $\dot{V}_o \le 0$ and Equation (23), the convergence condition of the observer is as follows:

$$\|\tilde{\varepsilon}\| \le \sqrt{\frac{\|\mathrm{X}\| \left(\left\|B\dot{g}\right\|^2 + \|H\|^2\right)}{\rho_{\min}(Q) - 2\|X\|}}. \tag{24}$$

Therefore, it is shown that the estimated $\tilde{\varepsilon}_1$, $\tilde{\varepsilon}_2$, $\tilde{\varepsilon}_3$ and $\tilde{\varepsilon}_4$ of the hyperbolic tangent extended state observer (9) is effective.□

3.2. Design of Fractional Order Global Sliding Mode Controller Based on Adaptive Fuzzy

For particleboard glue system, define the system ideal glue flow value as x_d, a fractional global sliding mode surface can be defined as:

$$s = \ddot{\xi} + \lambda_1 \dot{\xi} + \lambda_2 D^{-\beta} \xi + \lambda_3 \xi - P(t), \tag{25}$$

where $\xi = x_1 - x_d$, $\lambda_1 > 0$, $\lambda_2 > 0$, $\lambda_3 > 0$, $D^{-\beta}$ represents the fractional integral of the error used to eliminate the steady state error of the system. $P(t)$ is an exponential function to realize global sliding mode, and its expression is as follows:

$$P(t) = P(0) e^{-\chi t}, \tag{26}$$

where $\chi > 0$ and χ determines the convergence speed of $P(t)$; $P(0) = \ddot{\xi}(0) + \lambda_1 \dot{\xi}(0) + \lambda_2 {}_0D_0^{-\beta} \xi + \lambda_3 \xi(0)$, $\xi(0)$, $\dot{\xi}(0)$ and $\ddot{\xi}(0)$ are the initial error and its first and second derivatives, respectively. ${}_0D_0^{-\beta} \xi$ is fractional integral value at $t = 0$.

Then, the fractional order global integral sliding mode control law can be designed as

$$u_1 = -\frac{1}{b}\left[\hat{g} - \dddot{x}_d + \lambda_1\ddot{\hat{\xi}} + \lambda_2 D^{1-\beta}\hat{\xi} + \lambda_3\dot{\hat{\xi}} + P(0)\chi e^{-\chi t}\right] - \frac{1}{b}[\Upsilon(\hat{s}) + k\hat{s}], \tag{27}$$

where $\hat{g} = z_4$, $\hat{s} = \dddot{\hat{\xi}} + \lambda_1\ddot{\hat{\xi}} + \lambda_2 D^{-\beta}\hat{\xi} + \lambda_3\hat{\xi} - P(t)$, $\hat{\xi} = z_1 - x_d$, $\dot{\hat{\xi}} = z_2 - \dot{x}_d$, $\ddot{\hat{\xi}} = z_3 - \ddot{x}_d$, $\Upsilon(\hat{s}) = \eta\mathrm{sgn}(\hat{s})$, and $\eta > 0$, $k > 0$.

Motivated by the references [42,43], an adaptive fuzzy control method is introduced to fuzzy approximation of sliding mode switching term $\Upsilon(\hat{s})$, which can make the switching term continuous and reduce the chattering effect. A fuzzy logic system generally consists of four parts: the knowledge base, the fuzzifier, the fuzzy inference engine and defuzzifier. In this paper, the fuzzy inference engine uses a collection of the fuzzy IF-THEN rules to perform a mapping from input sliding variable vector to output vector. The design of fuzzy rules can be expressed as

$$\text{Rule } (j):\ \text{IF } \hat{s} \text{ is } A^j \text{ THEN } \hat{\Upsilon} \text{ is } B^j,\ (j = 1, 2, 3) \tag{28}$$

where $\hat{s}$ and $\hat{\Upsilon}$ are the input and output variables, respectively. A^j represents the input fuzzy set and B^j is the output fuzzy set corresponding to rule j. The expressions of S membership function and Gaussian membership function used to describe input fuzzy sets are as follows:

$$\mu_N(\hat{s}) = \frac{1}{1 + e^{-a_1(\hat{s} - c_1)}}, j = 1 \tag{29}$$

$$\mu_Z(\hat{s}) = e^{-(\hat{s} - c_2)^2/2\sigma^2}, j = 2 \tag{30}$$

$$\mu_P(\hat{s}) = \frac{1}{1 + e^{-a_2(\hat{s} - c_3)}}, j = 3 \tag{31}$$

where a_1, a_2, c_1 and c_3 are parameters of the S membership function, c_2 and σ represent the width and center of the Gaussian membership function, respectively.

The fuzzy system is designed by using product inference engine, single variable fuzzifier and central average defuzzifier, and the output $\hat{\Upsilon}(\hat{s})$ of the fuzzy system can be expressed as

$$\hat{\Upsilon}(\hat{s}) = \hat{\Upsilon}(\hat{s}|\phi) = \phi^T\varphi(\hat{s}) \tag{32}$$

where $\varphi(\hat{s})$ is a fuzzy vector, ϕ^T is the adjustable parameter vector of fuzzy approximator.

In an ideal case, $\hat{\Upsilon}(\hat{s}|\phi)$ can be represented as

$$\hat{\Upsilon}(\hat{s}|\phi^*) = \Upsilon(\hat{s}) = \eta\mathrm{sgn}(\hat{s}) \tag{33}$$

In order to improve the approximation ability of fuzzy system, the adaptive law is introduced to adjust the parameter vector ϕ, as shown below:

$$\dot{\hat{\phi}} = \gamma\hat{s}\varphi(\hat{s}) \tag{34}$$

where $\gamma > 0$.

Then, the $\hat{\Upsilon}(\hat{s})$ becomes

$$\hat{\Upsilon}(\hat{s}) = \hat{\Upsilon}(\hat{s}|\hat{\phi}) = \hat{\phi}^T\varphi(\hat{s}) \tag{35}$$

Then, the new control law can be obtained as follows:

$$u_1 = -\frac{1}{b}\left[\hat{g} - \dddot{x}_d + \lambda_1\ddot{\hat{\xi}} + \lambda_2 D^{1-\beta}\hat{\xi} + \lambda_3\dot{\hat{\xi}} + P(0)\chi e^{-\chi t}\right] - \frac{1}{b}[\hat{\Upsilon}(\hat{s}) + k\hat{s}] \tag{36}$$

4. Stability Analysis of Controller

Theorem 2. *Considering the system (6) with the novel hyperbolic tangent extended state observer designed early, if the fractional global sliding mode surface is chosen as (25), and the control law and adaptive law are designed as Equations (36) and (34), respectively, then the sliding mode surface s will gradually converge to 0 and the closed-loop system will be stable by selecting large enough parameter k and appropriate observer parameters l_1, l_2, l_3, l_4 and δ_1, δ_2, δ_3, δ_4.*

Proof of Theorem 2. Define the optimal parameters as follows:

$$\phi^* = \arg\min_{\hat{\phi}\in\Omega}\left[\sup\left|\hat{\Upsilon}(\hat{s}|\hat{\phi}) - \Upsilon(\hat{s})\right|\right] \tag{37}$$

where Ω is the aggregation of ϕ.

Choose the Lyapunov function for the controller as

$$V_s = \frac{1}{2}s^2 + \frac{1}{2}\frac{1}{\gamma}\tilde{\phi}^T\tilde{\phi} \tag{38}$$

where $\tilde{\phi} = \phi^* - \hat{\phi}$.

The derivation of Equation (38) can be obtained:

$$\begin{aligned}\dot{V}_s &= s\dot{s} + \tfrac{1}{\gamma}\tilde{\phi}^T\dot{\tilde{\phi}} \\ &= s\left[\dddot{\xi} + \lambda_1\ddot{\xi} + \lambda_2 D^{1-\beta}\xi + \lambda_3\dot{\xi} + P(0)\chi e^{-\chi t}\right] + \tfrac{1}{\gamma}\tilde{\phi}^T\dot{\tilde{\phi}}\end{aligned} \tag{39}$$

Considering Equations (8), (36) and (39), we can obtain

$$\begin{aligned}\dot{V}_s &= s\left[g - \hat{g} + v - \hat{v} - \hat{\Upsilon}(\hat{s}) - k\hat{s}\right] + \tfrac{1}{\gamma}\tilde{\phi}^T\dot{\tilde{\phi}} \\ &= s\left[\tilde{g} + \tilde{v} - \hat{\Upsilon}(\hat{s}|\hat{\phi}) + \hat{\Upsilon}(\hat{s}|\phi^*) - \hat{\Upsilon}(\hat{s}|\phi^*) - k\hat{s}\right] + \tfrac{1}{\gamma}\tilde{\phi}^T\dot{\tilde{\phi}} \\ &= s\left[\tilde{g} + \tilde{v} + \tilde{\phi}^T\varphi(\hat{s}) - \hat{\Upsilon}(\hat{s}|\phi^*) - k\hat{s}\right] - \tfrac{1}{\gamma}\tilde{\phi}^T\dot{\hat{\phi}}\end{aligned} \tag{40}$$

where $\tilde{g} = g - \hat{g}$, $g = x_4 = g(x_1, x_2, x_3, \omega(t), t)$, $\tilde{v} = v - \hat{v}$, $v = \lambda_1\ddot{\tilde{\xi}} + \lambda_2 D^{1-\beta}\xi + \lambda_3\dot{\xi}$, $\hat{v} = \lambda_1\ddot{\hat{\xi}} + \lambda_2 D^{1-\beta}\hat{\xi} + \lambda_3\dot{\hat{\xi}}$, $\tilde{\phi} = \phi^* - \hat{\phi}$, $\dot{\tilde{\phi}} = -\dot{\hat{\phi}}$.

According to the adaptive law (34), Equation (40) is expressed as

$$\dot{V}_s = s\left[\tilde{g} + \tilde{v} - \hat{\Upsilon}(\hat{s}|\phi^*) - k\hat{s}\right] + (s - \hat{s})\tilde{\phi}^T\varphi(\hat{s}) \tag{41}$$

Considering Equations (33) and (41), we can obtain

$$\dot{V}_s = s(\tilde{g} + \tilde{v}) + s[-\eta\mathrm{sgn}(\hat{s}) - k\hat{s}] + (s - \hat{s})\tilde{\phi}^T\varphi(\hat{s}) \tag{42}$$

Due to $s = \hat{s} + \tilde{s}$, $\dot{V}_s$ can be expressed as follows:

$$\begin{aligned}\dot{V}_s &= s(\tilde{g} + \tilde{v}) - \eta s\cdot\mathrm{sgn}(\hat{s}) - sk(s - \tilde{s}) + \tilde{s}\tilde{\phi}^T\varphi(\hat{s}) \\ &= -ks^2 + (\tilde{g} + \tilde{v} + k\tilde{s})s - \eta s\cdot\mathrm{sgn}(\hat{s}) + \tilde{s}\hat{\Upsilon}(\hat{s}|\tilde{\phi}) \\ &\le -ks^2 + (\tilde{g} + \tilde{v} + k\tilde{s})s + \eta|s| + |\tilde{s}|\left|\hat{\Upsilon}(\hat{s}|\tilde{\phi})\right|\end{aligned} \tag{43}$$

It can be seen that $\tilde{v}$, $\tilde{g}$ and $\tilde{s}$ in Equation (43) all depend on the estimation error of each state in the hyperbolic tangent extended state observer. Additionally, $\hat{\Upsilon}(\hat{s}|\tilde{\phi})$ depends on the approximation error of fuzzy controller. Therefore, we can find that $|\tilde{s}|\left|\hat{\Upsilon}(\hat{s}|\tilde{\phi})\right|$ is bounded.

Define $\Delta_{\max 1} \geq |\tilde{g} + \tilde{v} + k\tilde{s}|$, $\Delta_{\max 2} \geq |\tilde{s}|\left|\hat{\Upsilon}(\hat{s}|\tilde{\phi})\right|$, we can find that

$$\begin{aligned} \dot{V}_s &\leq -ks^2 + \Delta_{\max 1} s + \eta|s| + \Delta_{\max 2} \\ &\leq -ks^2 + \tfrac{1}{2}\left(\Delta_{\max 1}^2 + s^2\right) + \tfrac{1}{2}\left(\eta^2 + s^2\right) + \Delta_{\max 2} \\ &\leq -(k-1)s^2 + \tfrac{1}{2}\Delta_{\max 1}^2 + \Delta_{\max 2} \\ &= -(k-1)s^2 + \Delta \end{aligned} \tag{44}$$

where $\Delta = \frac{1}{2}\Delta_{\max 1}^2 + \Delta_{\max 2}$.

According to Equation (44), the controller can be stabilized by choosing a sufficiently large parameter $k > 1$ to make $\dot{V}_s(t) \leq 0$. Its convergence speed depends on the control gain k, the parameters of the observer and adaptive fuzzy approximator.

Considering the closed-loop system composed of hyperbolic tangent extended state observer and fuzzy fractional-order global sliding mode controller, Lyapunov function is defined as:

$$V = V_o + V_s \tag{45}$$

Derivation of V is as follows:

$$\begin{aligned} \dot{V} &= \dot{V}_o + \dot{V}_s \\ &\leq [-\rho_{\min}(Q) + 2\|\mathrm{X}\|]\|\tilde{\varepsilon}\|^2 + \|\mathrm{X}\|\left(\left\|B\dot{g}\right\|^2 + \|H\|^2\right) - (k-1)s^2 + \Delta \end{aligned} \tag{46}$$

According to Equation (46), $\dot{V} \leq 0$ can be guaranteed by selecting large enough k and appropriate parameters l_1, l_2, l_3, l_4 and δ_1, δ_2, δ_3, δ_4 and the convergence speed also depends on these parameters.□

5. Simulation Analysis

For particleboard glue system, in order to verify the effectiveness of adaptive fuzzy fractional-order global sliding mode controller based on hyperbolic tangent extended state observer, three simulation experiments were designed on Matlab2016/Simulink platform. In this simulation, the compound controller is designed according to Equations (9) and (36). In order to make the system output signal track, the desired signal more quickly and stably, the parameters are selected as follows:

(1) The parameters of hyperbolic tangent extended state observer are chosen as $l_1 = 60$, $l_2 = 120$, $l_3 = 700$, $l_4 = 1200$, $\delta_1 = 1$, $\delta_2 = 0.01$, $\delta_3 = 0.002$, $\delta_4 = 0.00004$, and initial values of observer are $z_1 = z_2 = z_3 = z_4 = 0$.

(2) The fractional order global sliding mode controller parameters are chosen as $\lambda_1 = 8$, $\lambda_2 = 0.05$, $\lambda_3 = 18$, $k = 10$, $P(t) = P(0)e^{-100t}$, where $P(0) = -10$.

(3) The membership functions of switching function s are defined as $\mu_N(s) = \frac{1}{1+e^{5(s+20)}}$, $\mu_Z(s) = \frac{1}{e^{-s^2}}$, $\mu_P(s) = \frac{1}{1+e^{5(s-20)}}$, and the adaptive parameter are chosen as $\gamma = 100$.

(4) The desired glue flow is $y_d = 10\mathrm{L/min}$, The initial value of the system states are defined as $x_1 = 0$, $x_2 = 0$, $x_3 = 0$, $x_4 = 0$, and the compound disturbance is chosen as $\omega(t) = 10\sin(t)$.

Compared with sliding mode control (SMC), fractional sliding mode control (FOSMC) and fractional order global sliding mode control (FOGSMC) method, the simulation results are shown in Figures 5–8.

The time response of desired glue flow signal tracking and tracking error is shown in Figure 5. It is clearly shown that the control method proposed in this paper is much faster than the traditional sliding mode control, fractional order sliding mode control and fractional order global sliding mode control, which can realize the fast, accurate and no overshoot tracking of the glue flow. In addition, it is clear that fractional calculus can improve the ability of fast response of the system.

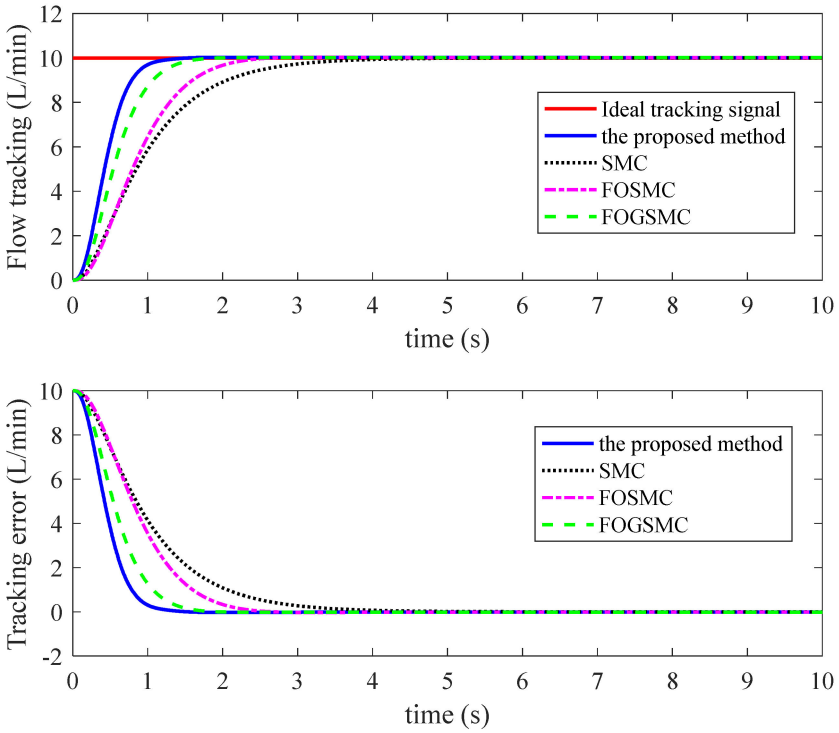

Figure 5. Time response of glue flow tracking and tracking error.

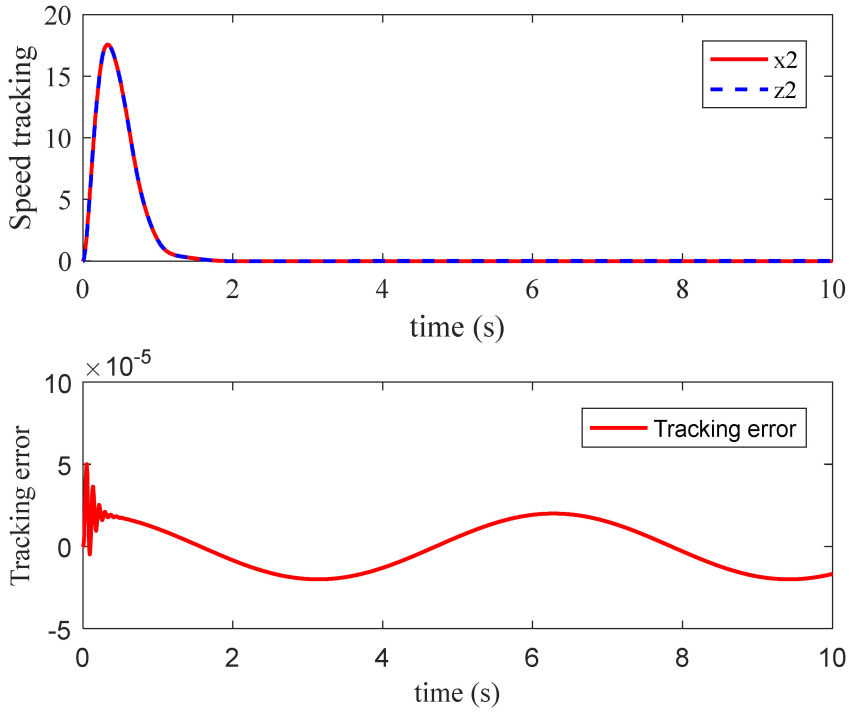

Figure 6. Time response and tracking error of observer for speed tracking. (x_2 and z_2 represent the practical speed state of the system and the corresponding state estimated by the observer, respectively).

Figures 6–8 show the tracking performance of the hyperbolic tangent extended state observer for system states and total disturbances. It can be obtained that the tracking accuracy of the observer to the speed state of the system can reach 5×10^{-5}, and the tracking accuracy to the acceleration state of the system is about 5×10^{-3}. In addition, although the total disturbance estimation error caused by the input signal jump at the initial time is

large, the observer designed in this paper can quickly track the disturbance signal, which shows the hyperbolic tangent extended state observer has good estimation performance.

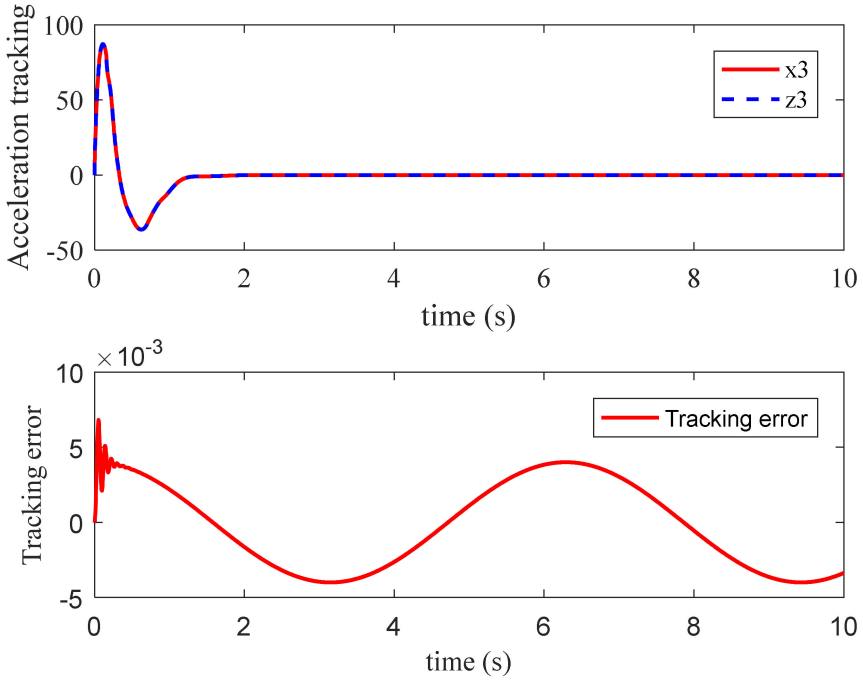

Figure 7. Time response and tracking error of observer for acceleration tracking. (x_3 and z_3 represent the practical acceleration state of the system and the corresponding state estimated by the observer, respectively).

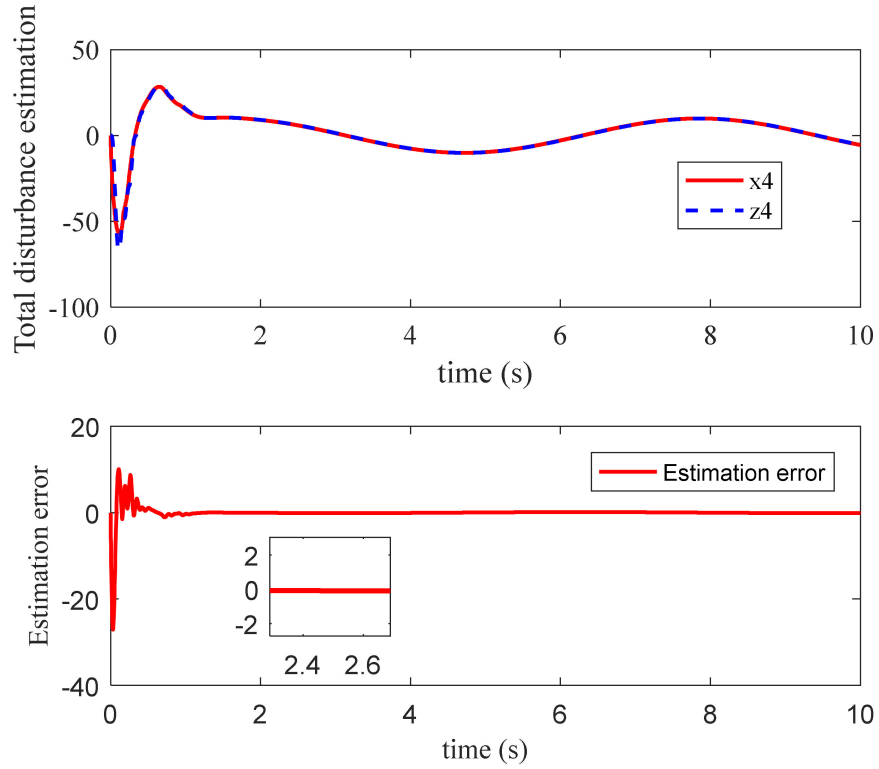

Figure 8. Time response and estimation error of observer for total disturbance. (x_4 and z_4 represent the practical total disturbance of the system and the corresponding state estimated by the observer, respectively).

In order to further verify the control effect of the proposed method, the ideal glue flow signal is set as a square wave signal with an amplitude of 10 and the total disturbance of the system is selected as the fitting model from the Reference [44], whose expression is $\omega(t) = 50\sin(t) + 40\cos(t) + 100e^{-2(t-5)^2}$. The simulation results of the system response are shown in Figures 9–13.

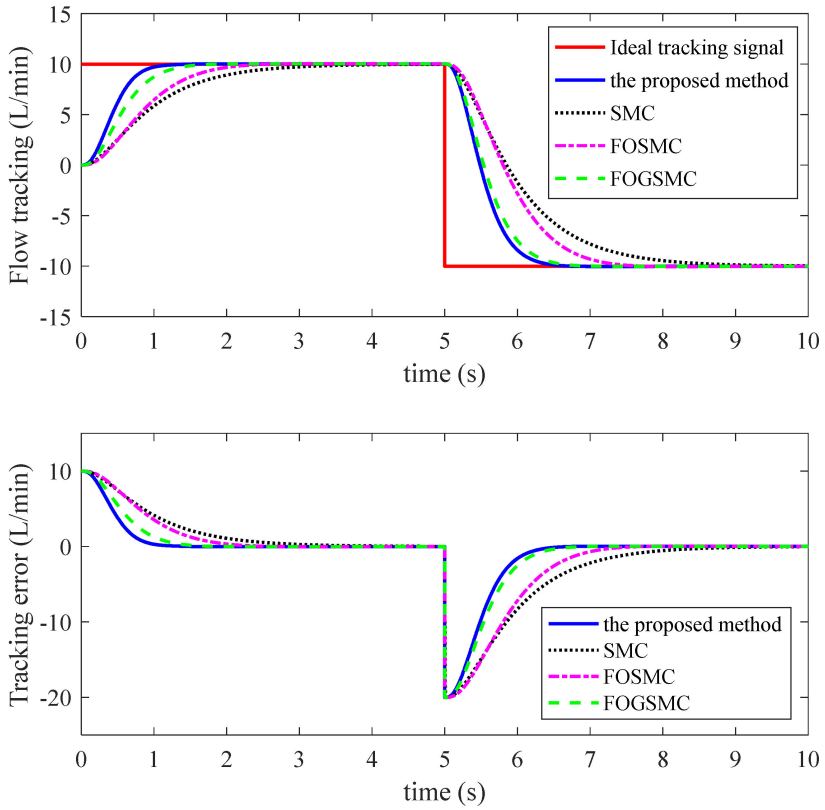

Figure 9. Time response of glue flow tracking and tracking error.

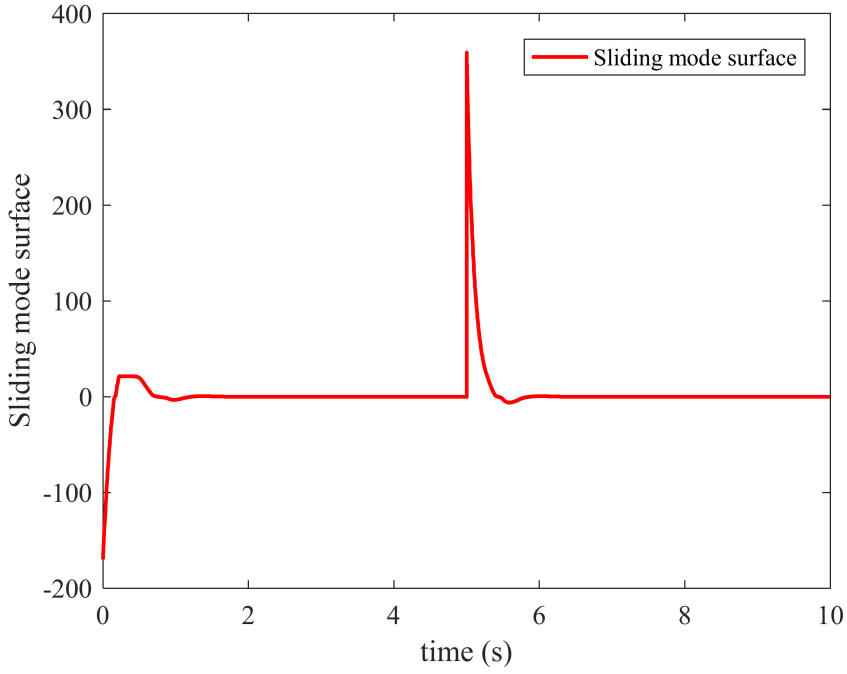

Figure 10. Time response of sliding mode surface.

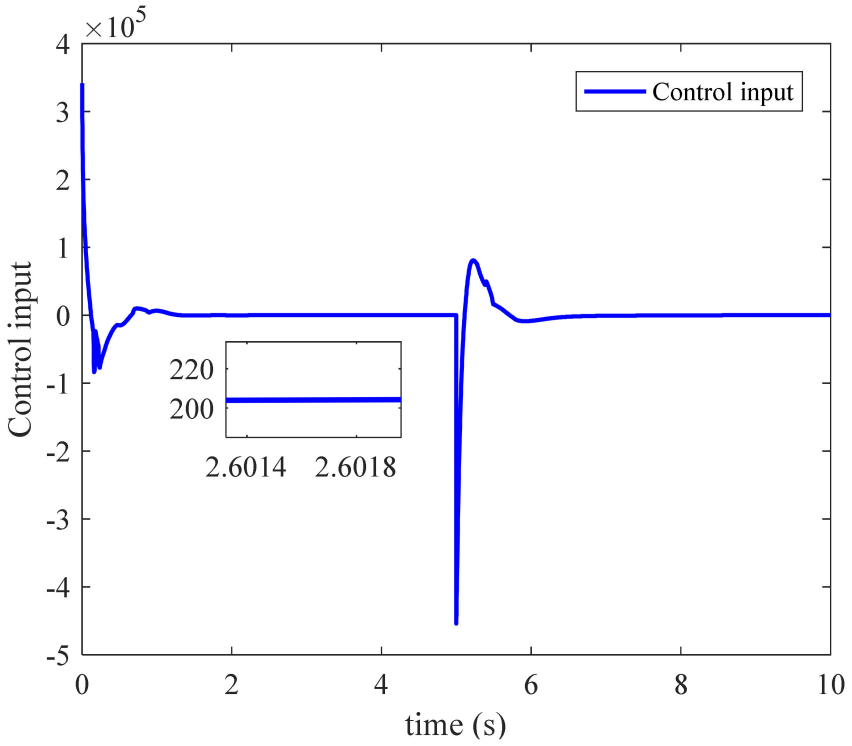

Figure 11. Time response of the control input.

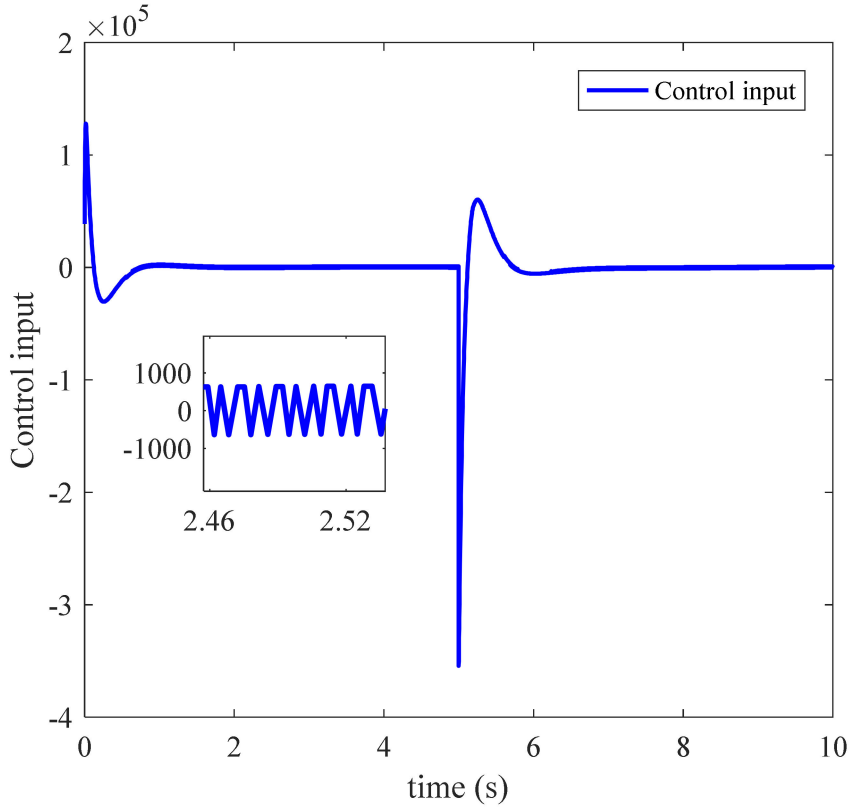

Figure 12. Time response of control input without adaptive fuzzy control.

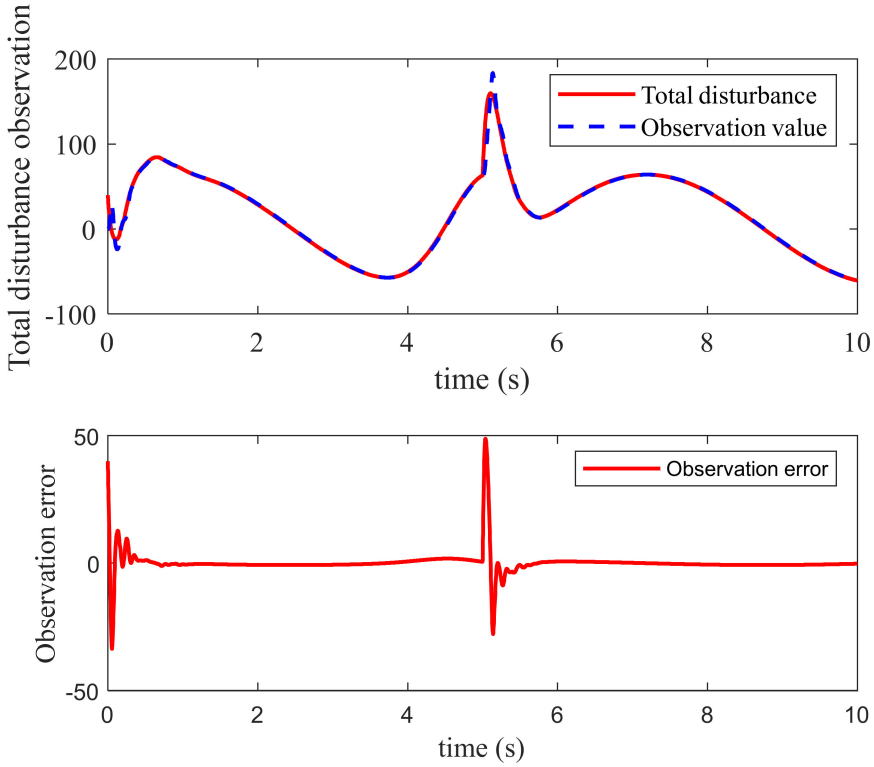

Figure 13. Time response of total disturbance observation.

It can be clearly seen from Figure 9 that the proposed method can still track the desired glue flow quickly, accurately and without overshoot when the system inputs a changing square wave signal, which fully demonstrates the good control performance of the designed controller.

Figures 10 and 11 are the time response curves of sliding mode surface and control input of the proposed controller, respectively. Figure 12 is the time response curve of control input without adaptive fuzzy controller. It can be clearly shown that the sliding mode surface of the controller designed in this paper can quickly converge to 0. After adding the adaptive fuzzy approximator, the chattering phenomenon of the system can be greatly reduced and the control performance of the system can be improved.

The disturbance observation curve shown in Figure 13 shows that the hyperbolic tangent extended state observer can observe the disturbance well.

In order to simulate the influence of actual working conditions, the random noise disturbance is considered as the total disturbance of the system to verify the effectiveness of the proposed control scheme, and the simulation results are shown in Figures 14 and 15.

Through the analysis of the simulation results, the effectiveness of the method is proved, including the ability to track the desired signal quickly and accurately and the robustness to complex interference.

Remark 2. *In the previous work Reference [4], an improved ADRC controller is designed to solve the time-delay problem by a neural network state observer, and the traditional sliding mode control is used to ensure the robustness of the system. In Reference [5], a prescribed performance control method is used to improve the transient behavior and the disturbance is observed by normal ESO. In this paper, we use the hyperbolic tangent function to improve the extended state observer and obtain high estimation accuracy, and focus on the combination of fractional operator and sliding mode control to improve the rapidity of the system. Furthermore, the proposed control strategy employs an adaptive fuzzy control law to weaken chattering, which is also not addressed in previous work.*

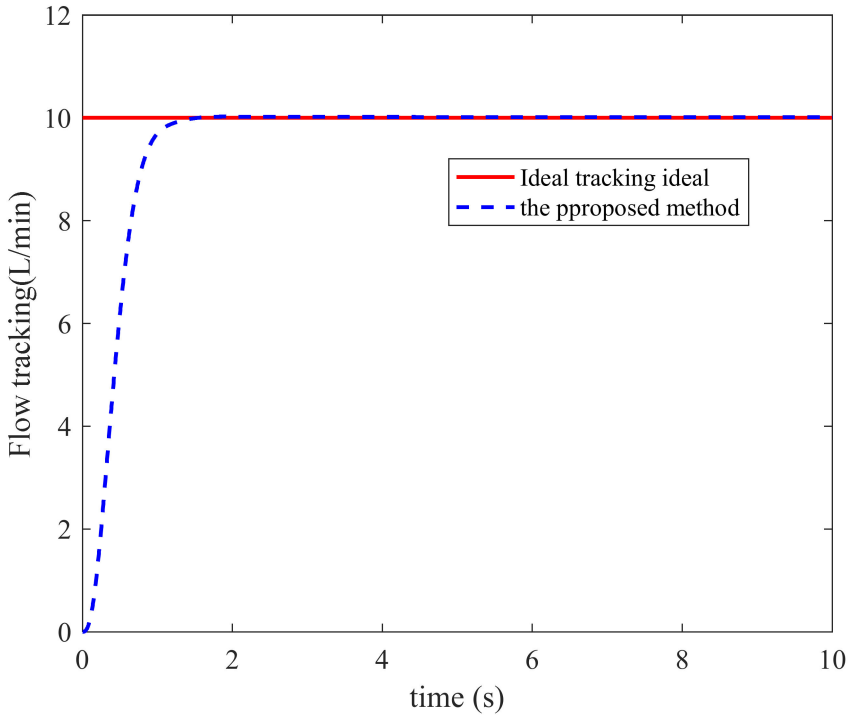

Figure 14. Time response of glue flow tracking.

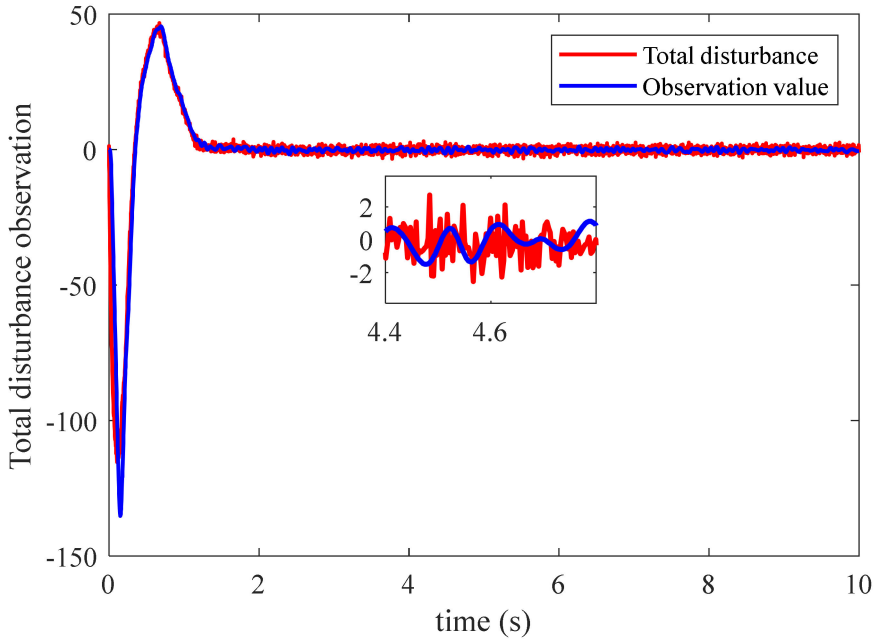

Figure 15. Time response of total disturbance observation.

6. Conclusions

In order to solve the problems of time delay, complex disturbance and unmeasurable system state caused by glue pipe, external disturbance, motor and pump inertia, a new compound control algorithm based on hyperbolic tangent extended state observer and adaptive fuzzy fractional order global sliding mode controller is proposed. A hyperbolic tangent function is introduced into the extended state observer to improve the estimation ability for system states and complex disturbances. The fractional global sliding mode controller based on exponential reaching law is used to accelerate the convergence speed and improve the control performance of the system. In addition, an adaptive fuzzy controller

is introduced to approximate the sliding mode switching term, which greatly reduces the chattering phenomenon of the system. Moreover, the convergence of the proposed observer and the controller are proved through rigorous Lyapunov analysis. Finally, through the numerical simulation experiment, and compared with the traditional SMC, FOSMC and FODSMC strategies, it is verified that the proposed control method has the excellent performance of fast response, high control accuracy and good robustness.

Considering that the plant in this paper is an identification model, we will focus on exploring model building and performance evaluation of control algorithms on real platforms in future research.

Author Contributions: Conceptualization and methodology, X.Q.; validation, X.Q.; writing—original draft preparation, P.W. and L.Z.; writing—review and editing, P.W. and L.Z. All authors have read and agreed to the published version of the manuscript.

Funding: This research was funded by Fundamental Research Funds of Central Universities (2572018BF02), National Natural Science Foundation of China (31370710), the 948 Project from the Ministry of Forestry of China (2014-4-46).

Data Availability Statement: Not applicable.

Acknowledgments: The authors thank the anonymous reviewers for their useful comments that improved the quality of the paper.

Conflicts of Interest: The authors declare no conflict of interest.

References

1. Uemura Silva, V.; Nascimento, M.F.; Resende Oliveira, P.; Panzera, T.H.; Rezende, M.O.; Silva, D.A.L.; Borges de Moura Aquino, V.; Rocco Lahr, F.A.; Christoforo, A.L. Circular vs. linear economy of building materials: A case study for particleboards made of recycled wood and biopolymer vs. conventional particleboards. *Constr. Build. Mater.* **2021**, *285*, 122906. [CrossRef]
2. Kariuki, S.W.; Wachira, J.; Kawira, M.; Murithi, G. Crop residues used as lignocellulose materials for particleboards formulation. *Heliyon* **2020**, *6*, e05025. [CrossRef] [PubMed]
3. Saravia-Cortez, A.M.; Herva, M.; García-Diéguez, C.; Roca, E. Assessing environmental sustainability of particleboard production process by ecological footprint. *J. Clean. Prod.* **2013**, *52*, 301–308. [CrossRef]
4. Wang, P.; Zhang, C.; Zhu, L.; Wang, C. The Research of Improved Active Disturbance Rejection Control Algorithm for Particleboard Glue System Based on Neural Network State Observer. *Algorithms* **2019**, *12*, 259. [CrossRef]
5. Wang, P.; Zhu, L.; Zhang, C.; Wang, C.; Xiao, K. Prescribed Performance Control with Sliding-Mode Dynamic Surface for a Glue Pump Motor Based on Extended State Observers. *Actuators* **2021**, *10*, 282. [CrossRef]
6. Hui, T.; Zeng, W.; Yu, T. Core power control of the ADS based on genetic algorithm tuning PID controller. *Nucl. Eng. Des.* **2020**, *370*, 110835. [CrossRef]
7. Miranda-Colorado, R.; Aguilar, L.T. Robust PID control of quadrotors with power reduction analysis. *ISA Trans.* **2020**, *98*, 47–62. [CrossRef]
8. Jakub, B.; Jakub, K. Active Disturbance Rejection Control for Dielectric Electroactive Polymer Actuator. *IEEE Access* **2021**, *9*, 95218–95227. [CrossRef]
9. Chen, Y.; Zhu, P.; Zhang, P.; Li, M.; Zhang, W. Hybrid Sliding Mode Position Tracking Control for Servo System with External Disturbance. *IEEE J. Emerg. Sel. Top. Power Electron.* **2021**, *9*, 5478–5488. [CrossRef]
10. Guo, J. Application of a novel adaptive sliding mode control method to the load frequency control. *Eur. J. Control.* **2021**, *57*, 172–178. [CrossRef]
11. Zhang, H.; Wang, T. Finite-Time Sliding Mode Control for Uncertain Neutral Systems With Time Delays. *IEEE Access* **2021**, *9*, 140446–140455. [CrossRef]
12. Chang, W.; Li, Y.; Tong, S. Adaptive Fuzzy Backstepping Tracking Control for Flexible Robotic Manipulator. *IEEE/CAA J. Autom. Sin.* **2021**, *8*, 1923–1930. [CrossRef]
13. Li, Z.; Wang, F.; Ke, D.; Li, J.; Zhang, W. Robust Continuous Model Predictive Speed and Current Control for PMSM With Adaptive Integral Sliding-Mode Approach. *IEEE Trans. Power Electron.* **2021**, *36*, 14398–14408. [CrossRef]
14. Liu, W.; Zhao, T. An active disturbance rejection control for hysteresis compensation based on Neural Networks adaptive control. *ISA Trans.* **2021**, *109*, 81–88. [CrossRef]
15. Lin, F.; Chen, C.; Xiao, G.; Chen, P. Voltage Stabilization Control for Microgrid With Asymmetric Membership Function-Based Wavelet Petri Fuzzy Neural Network. *IEEE Trans. Smart Grid* **2021**, *12*, 3731–3741. [CrossRef]
16. Omid, M.; Saleh, M.; Afef, F. Adaptive Integral-Type Terminal Sliding Mode Control for Unmanned Aerial Vehicle Under Model Uncertainties and External Disturbances. *IEEE Access* **2021**, *9*, 53255–53265. [CrossRef]

17. Hu, C.; Wu, D.; Liao, Y.; Hu, X. Sliding mode control unified with the uncertainty and disturbance estimator for dynamically positioned vessels subjected to uncertainties and unknown disturbances. *Appl. Ocean. Res.* **2021**, *109*, 102564. [CrossRef]
18. Xiao, X.; Lv, J.; Chang, Y.; Chen, J.; He, H. Adaptive Sliding Mode Control Integrating with RBFNN for Proton Exchange Membrane Fuel Cell Power Conditioning. *Appl. Sci.* **2022**, *12*, 3132. [CrossRef]
19. Nguyen, M.H.; Dao, H.V.; Ahn, K.K. Adaptive Robust Position Control of Electro-Hydraulic Servo Systems with Large Uncertainties and Disturbances. *Appl. Sci.* **2022**, *12*, 794. [CrossRef]
20. Mourad, A.; Youcef, Z. Adaptive Sliding Mode Control Improved by Fuzzy-PI Controller: Applied to Magnetic Levitation System. *Eng. Proc.* **2022**, *14*, 14. [CrossRef]
21. Chang, E.-C.; Cheng, H.-L.; Chang, C.-H.; Wu, R.-C.; Cheng, C.-A.; Xiao, Z.-K.; Lu, W.-J.; Wei, Z.-Y. Robust Optimal Control Design for Performance Enhancement of PWM Voltage Source Inverter. *Micromachines* **2022**, *13*, 435. [CrossRef] [PubMed]
22. Firouzi, B.; Alattas, K.A.; Bakouri, M.; Alanazi, A.K.; Mohammadzadeh, A.; Mobayen, S.; Fekih, A. A Type-2 Fuzzy Controller for Floating Tension-Leg Platforms in Wind Turbines. *Energies* **2022**, *15*, 1705. [CrossRef]
23. Pan, Q.; Li, X.; Fei, J. Adaptive Fuzzy Neural Network Harmonic Control with a Super-Twisting Sliding Mode Approach. *Mathematics* **2022**, *10*, 1063. [CrossRef]
24. Huang, J.-T.; Chiu, C.-K. Adaptive Fuzzy Sliding Mode Control of Omnidirectional Mobile Robots with Prescribed Performance. *Processes* **2021**, *9*, 2211. [CrossRef]
25. Ding, Y.; Wang, X.; Bai, Y.; Cui, N. Global smooth sliding mode controller for flexible air-breathing hypersonic vehicle with actuator faults. *Aerosp. Sci. Technol.* **2019**, *92*, 563–578. [CrossRef]
26. Boukattaya, M.; Gassara, H.; Damak, T. A global time-varying sliding-mode control for the tracking problem of uncertain dynamical systems. *ISA Trans.* **2020**, *97*, 155–170. [CrossRef]
27. Wang, H.; Wu, S.; Wang, Q. Global Sliding Mode Control for Nonlinear Vehicle Antilock Braking System. *IEEE Access* **2021**, *9*, 40349–40359. [CrossRef]
28. Wang, T.; Tan, N.; Qiu, J.; Yu, Y.; Zhang, X.; Zhai, Y.; Labati, R.; Piuri, V.; Scotti, F. Global-Equivalent Sliding Mode Control Method for Bridge Crane. *IEEE Access* **2021**, *9*, 160372–160382. [CrossRef]
29. Yang, Z.; Ding, Q.; Sun, X.; Zhu, H.; Lu, C. Fractional-order sliding mode control for a bearingless induction motor based on improved load torque observer. *J. Frankl. Inst.* **2021**, *358*, 3701–3725. [CrossRef]
30. Silaa, M.Y.; Barambones, O.; Derbeli, M.; Napole, C.; Bencherif, A. Fractional Order PID Design for a Proton Exchange Membrane Fuel Cell System Using an Extended Grey Wolf Optimizer. *Processes* **2022**, *10*, 450. [CrossRef]
31. Sami, I.; Ullah, S.; Ali, Z.; Ullah, N.; Ro, J.-S. A Super Twisting Fractional Order Terminal Sliding Mode Control for DFIG-Based Wind Energy Conversion System. *Energies* **2020**, *13*, 2158. [CrossRef]
32. Sami, I.; Ullah, S.; Ullah, N.; Ro, J.-S. Sensorless fractional order composite sliding mode control design for wind generation system. *ISA Trans.* **2021**, *111*, 275–289. [CrossRef]
33. Xiong, L.; Li, P.; Ma, M.; Wang, Z.; Wang, J. Output power quality enhancement of PMSG with fractional order sliding mode control. *Int. J. Electr. Power Energy Syst.* **2020**, *115*, 105402. [CrossRef]
34. Cuong, H.M.; Dong, H.Q.; Trieu, P.V.; Tuan, L.A. Adaptive fractional-order terminal sliding mode control of rubber-tired gantry cranes with uncertainties and unknown disturbances. *Mech. Syst. Signal Process.* **2021**, *154*, 107601. [CrossRef]
35. Zhu, P.; Chen, Y.; Li, M.; Zhang, P.; Wan, Z. Fractional-order sliding mode position tracking control for servo system with disturbance. *ISA Trans.* **2020**, *105*, 269–277. [CrossRef]
36. Wu, X.; Huang, Y. Adaptive fractional-order non-singular terminal sliding mode control based on fuzzy wavelet neural networks for omnidirectional mobile robot manipulator. *ISA Trans.* **2021**, *121*, 258–267. [CrossRef]
37. Zhuang, H.; Sun, Q.; Chen, Z.; Jiang, Y. Back-stepping sliding mode control for pressure regulation of oxygen mask based on an extended state observer. *Automatica* **2020**, *119*, 109106. [CrossRef]
38. Zhao, L.; Liu, X.; Wang, T. Trajectory tracking control for double-joint manipulator systems driven by pneumatic artificial muscles based on a nonlinear extended state observer. *Mech. Syst. Signal Process.* **2019**, *122*, 307–320. [CrossRef]
39. Zhao, Z.-L.; Guo, B.-Z. A nonlinear extended state observer based on fractional power functions. *Automatica* **2017**, *81*, 286–296. [CrossRef]
40. Chen, J.; Sun, L.; Sun, G.; Li, Y.; Zhu, B. Generalized predictive tracking control of spacecraft attitude based on hyperbolic tangent extended state observer. *Adv. Space Res.* **2020**, *66*, 335–344. [CrossRef]
41. Guo, J.; Cao, J.; Fu, Y.; Ma, Z.; Li, B.; Liu, D. Flow tracking of glue system based on non-singular terminal sliding mode active disturbance rejection control. *ICIC Int.* **2020**, *16*, 1757–1768.
42. Bahtiyar, B. Real-time analysis of adaptive fuzzy predictive controller for chaotification under varying payload and noise conditions. *Neural Comput. Appl.* **2021**, *33*, 13449–13465. [CrossRef]
43. Mao, W.-L.; Chiu, Y.-Y.; Lin, B.-H.; Sun, W.-C.; Tang, J.-F. Direct Fuzzy CMAC Sliding Mode Trajectory Tracking for Biaxial Position System. *Energies* **2021**, *14*, 7802. [CrossRef]
44. Liu, D.; Cao, J. Cascade control of particleboard supplying glue based on Smith predictor. *J. Comput. Inf. Syst.* **2008**, *4*, 2033–2038.